Unusual donor-acceptor system $Mn^{II}Pc$-TCNQ/F_4-TCNQ and the properties of the mixed single crystals of the metal phthalocyanines with organic acceptor molecules

Olga Kataeva,*[a] Kirill Metlushka,[a] Kamil Ivshin,[a,b] Kristina Nikitina,[a] Vladimir Alfonsov,[a] Alexander Vandyukov,[a] Mikhail Khrizanforov,[a] Yulia Budnikova,[a] Oleg Sinyashin,[a] Yulia Krupskaya,[c] Vladislav Kataev,[c] Bernd Büchner,[c,d] and Martin Knupfer[c]

[a]Arbuzov Institute of Organic and Physical Chemistry, FRC Kazan Scientific Center, Russian Academy of Sciences, Arbuzov str. 8, 420088 Kazan, Russia.

[b]A.M. Butlerov Chemistry Institute of the Kazan Federal University, Kremlevskaya str. 18, 420008 Kazan, Russia.

[c]Institute for Solid State and Materials Research IFW Dresden, Helmholtz str. 20, 01069 Dresden, Germany.

[d]Institut für Feskörper- und Materialphysik, Technische Universität Dresden, 01062 Dresden, Germany.

Electronic Supplementary Information

Table of contents:

1. DSC measurements

DSC-thermogramms and thermochemistry parameters (fusion temperature and enthalpy) of **1a**, **1b** and **2** are shown in Figure S1-S3. The DSC studies of the complexes indicate the decomposition of the samples upon heating, apparently, with the loss of crystallization water and solvate DMPU or DMAC molecules.

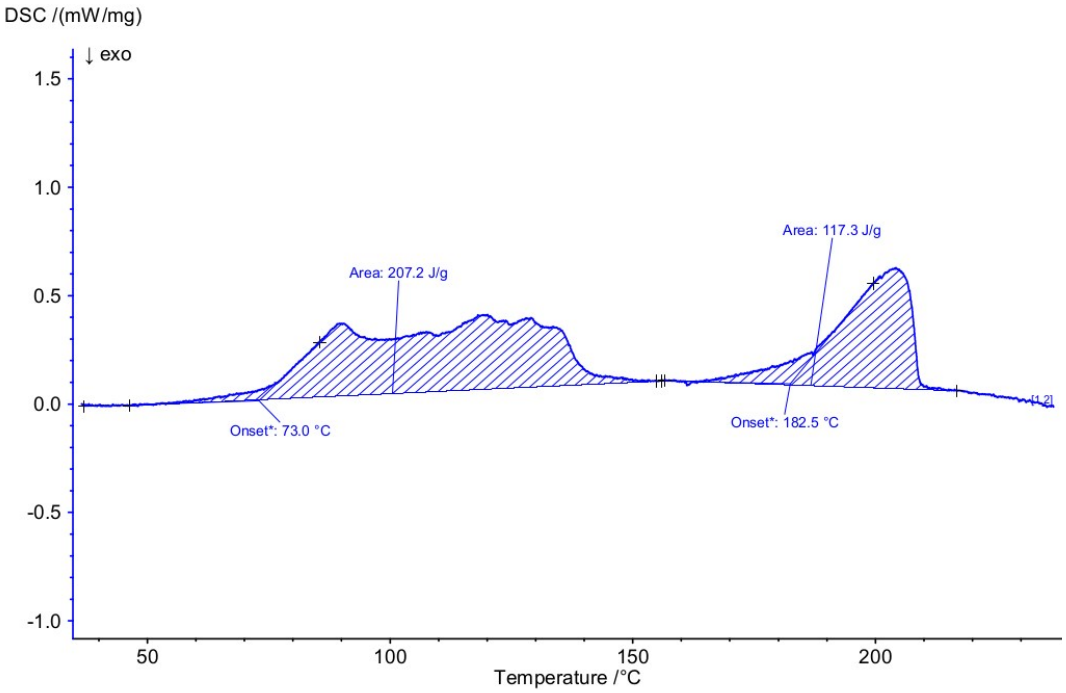

Figure S1. DSC thermogram of **1a**.

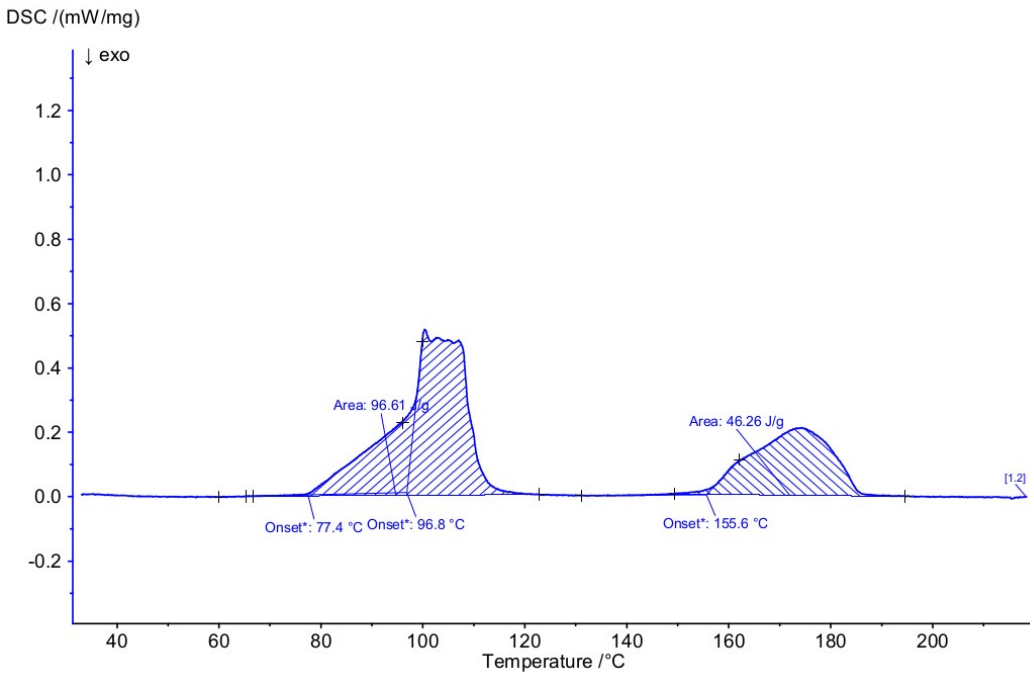

Figure S2. DSC thermogram of **1b**.

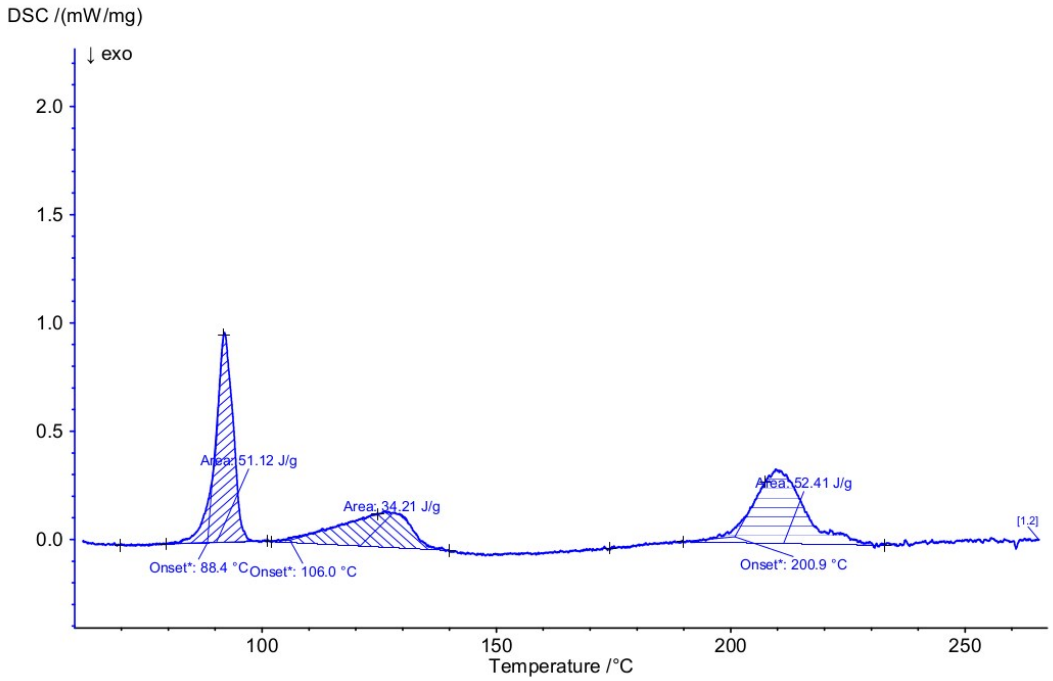

Figure S3. DSC thermogram of **2**.

2. IR spectroscopy

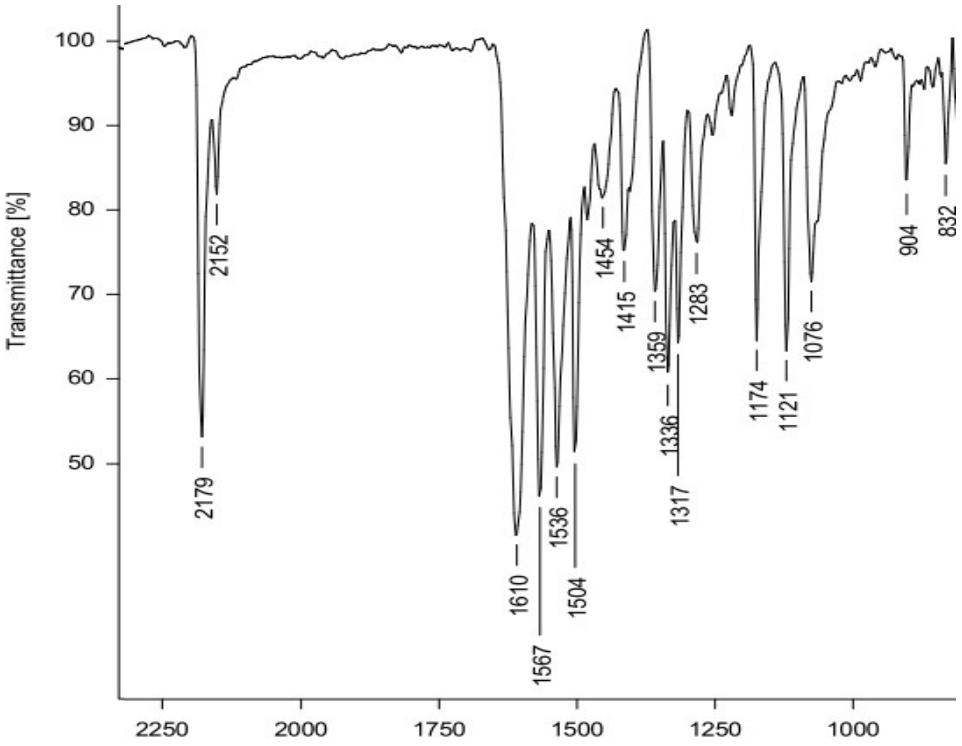

Figure S4. A fragment of the IR spectrum of **1a**.

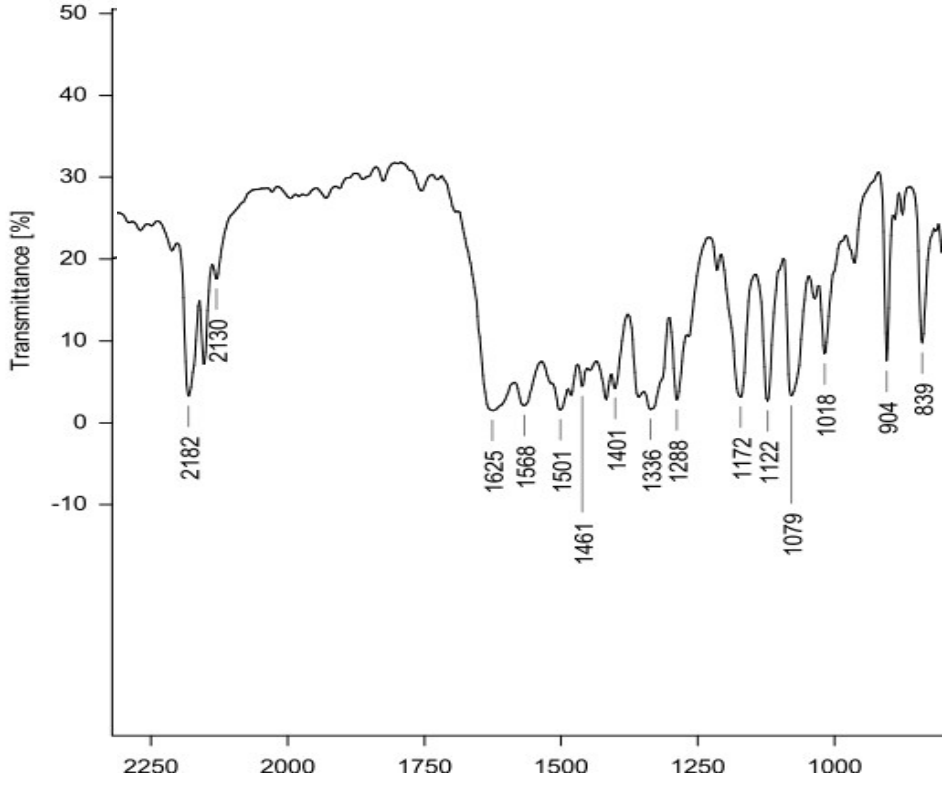

Figure S5. A fragment of the IR spectrum of **1b**.

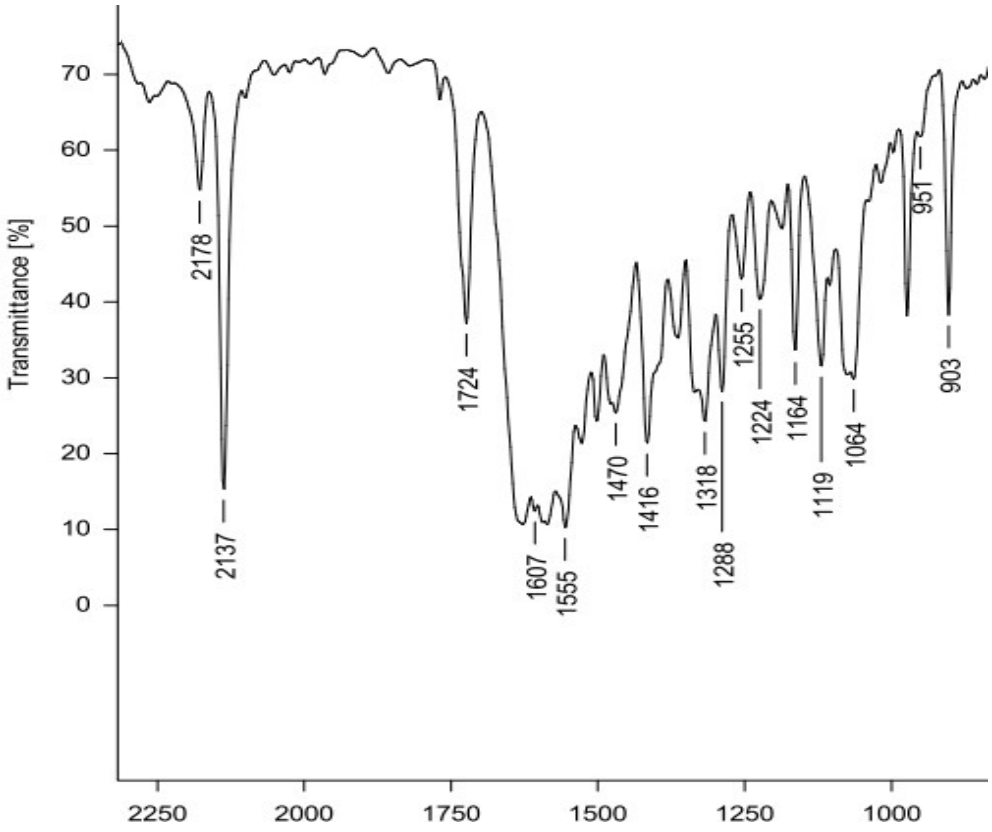

Figure S6. A fragment of the IR spectrum of **2**.

3. Crystallographic Data

Table S1. Crystal data for compounds 1a, 1b and 2.

Compound	Crystal **1a**	Crystal **1b**	Crystal **2**
CCDC number	1940628	1940630	1940627
Empirical formula	$C_{68}H_{72}MnN_{20}O_6$	$C_{60}H_{60}MnN_{16}O_6$	$C_{68}H_{68}F_4MnN_{20}O_6$
Formula weight [g/mol]	1320.39	1156.18	1392.36
Temperature [K]	100(2)	100(2)	198(2)
Wavelength [Å]	0.71073	0.71073	1.54178
Crystal system	Triclinic	Triclinic	Triclinic
Space group	P-*1*	P-*1*	P-*1*
Unit cell dimensions			
a [Å]	8.7610(8)	8.5252(5)	8.7022(2)
b [Å]	11.1909(10)	10.6614(7)	11.6296(3)
c [Å]	17.2255(15)	16.8696(10)	16.8340(4)
α [°]	71.657(6)	74.183(4)	74.6000(10)°
β [°]	76.151(5)	75.806(3)	79.8630(10)°
γ [°]	87.937(6)	85.511(4)	89.0450(10)°
Volume	1555.0(2)	1430.09(16)	1616.03(7)
Z	1	1	1
Density [g cm^{-3}]	1.410	1.342	1.431
Absorption coefficient, mm^{-1}	0.285	0.298	2.354
F(000)	693	605	725
Crystal size [mm^3]	0.222 x 0.183 x 0.040	0.683 x 0.361 x 0.120	0.231 x 0.093 x 0.043
Θ range for data collection	2.567 to 27.958	2.581 to 28.408	2.767 to 66.641
Limiting indices	-11<=*h*<=11, -14<=*k*<=14, -22<=*l*<=22	-11<=*h*<=11, -14<=*k*<=14, -22<=*l*<=22	-10<=*h*<=10, -13<=*k*<=13, -20<=*l*<=20
Reflections collected	30426	46196	19514
Independent reflections	7287 [R(int) = 0.0758]	7133 [R(int) = 0.1193]	5632 [R(int) = 0.0603]
Completeness, %	97.8	99.5	98.6
Data / restraints / parameters	7287/ 0 / 442	7133 / 126 / 457	5632 / 0 / 470
Goodness-of-fit on F2	1.037	1.015	1.056
Final R indices [I>2sigma(I)]	R1 = 0.0638, wR2 = 0.1444	R1 = 0.0707, wR2 = 0.1634	R1 = 0.0572, wR2 = 0.1644
R indices (all data)	R1 = 0.1050, wR2 = 0.1651	R1 = 0.1441, wR2 = 0.2006	R1 = 0.0677, wR2 = 0.1779
Largest diff. peak and hole [e.$Å^{-3}$]	0.940 (-0.433)	0.502(-0.596)	0.667 (-0.549)

The crystals **1b** and **2** contain statistically disordered solvent molecules, thus sharp decrease of the reflections' intensity is observed. In spite of the comparatively large exposure time the ratio of observed to collected reflections does not exceed 60% for the Mo-radiation data set of crystal **1b**. For single crystal **2** the data set was collected using Cu-radiation.

However, even the 60 s per frame exposure time for higher theta images showed no observed reflections at resolution higher than 1.0 Å (see Fig. S7).

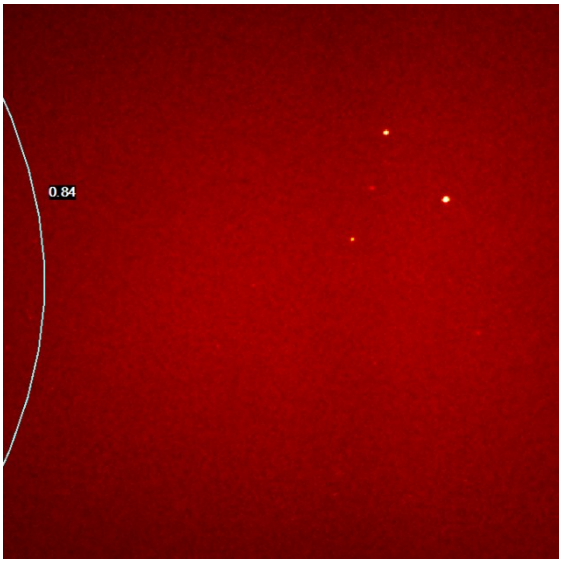

Figure S7. Typical diffraction image in the 2theta range from 63-135° for crystal **2**.

Several crystal growth experiments in various conditions (variable temperature, concentration, solvents) were performed to achieve better crystal quality. All experiments produced the same crystals of similar quality, the best being chosen for the data collection. Due to the flaws mentioned above, the refinement of the crystals resulted in the problems which should be addressed, such as the depletion of electron density around the fluorine atoms in crystal **2** (Fig. S8), located outside the molecular plane. The refinement of the occupancy of the fluorine atoms produced the value close to 0.9 with a slight decrease of the R-factor. One can see much larger thermal vibrational parameters of fluorine atoms in comparison with the carbon atoms of the ring, which might indicate possible disorder or vibrations in the direction perpendicular to the molecular plane. However all the bond lengths have "normal" values for the fully occupied model of the acceptor molecule. Similar problems were encounted in the refinement of structure **1b**, which showed lower occupancy of the terminal nitrogen atoms in acceptor molecule. It is worth mentioning, that the crystal **1a** exhibits no disorder and diffracted well in a whole 2theta range, as a result the structure was refined without the problems observed for crystals **1b** and **2**, which indirectly provides the additional proof for the correct structure model in crystals **1b** and **2**.

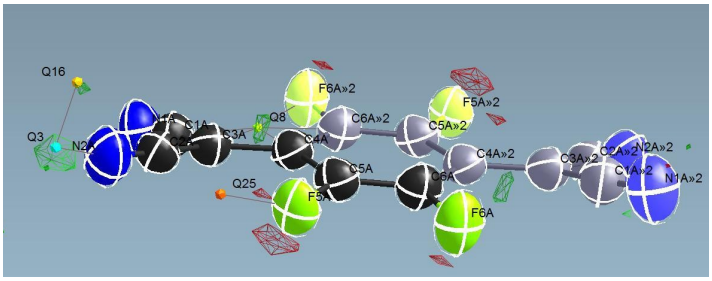

Figure S8. The ORTEP drawing of acceptor molecule in crystal **2**, showing the depletion of electron density in the vicinity of fluorine atoms (red color).

In spite of encounted refinement problems, the geometry of acceptor molecules gave reasonable values for charge transfer degree. The charge transfer degree was estimated using Kistenmacher formula. The parameters A1 and A2 in the formula (Table S2) are empirically derived from the geometry of neutral TCNQ/F_4-TCNQ molecules and their anions.[1]

Table S2. Selected bond lengths and estimated charge transfer degree δ.

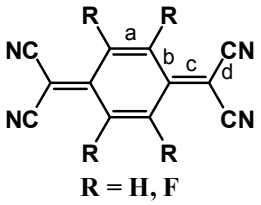

R = H, F

$$\delta = A_1 \frac{c}{b+d} - A_2$$

	1a T = 100K	**1b** T = 100K	**2** T = 198K
a	1.357(5)	1.358(6)	1.358(5)
b	1.417(5)	1.421(6)	1.411(5)
c	1.404(5)	1.398(7)	1.410(5)
d	1.407(5)	1.366(7)	1.418(5)
δ	0.90	1.08	0.96

Crystallographic data for the crystal structures have been deposited with the Cambridge Crystallographic Data Centre as supplementary publication no. 1940627, 1940628 and 1940630. Copies of the data can be obtained free of charge on application to CCDC, 12 Union Road, Cambridge CB2 1EZ, UK (fax: (+44)1223-336-033; e-mail: deposit@ccdc.cam.ac.uk, http://www.ccdc.cam.ac.uk).

[1] F. H. Herbstein, *Crystalline Molecular Complexes and Compounds: Structures and Principles*, 1 edition, Oxford University Press, 2006.

4. Electrochemical Measurements

Electrochemical parameters for $Mn^{III}PcQ^{-}$ and its precursor are given in Table S3. The first reduction potential refers to the change of Mn^{III} to Mn^{II}, the next peak is associated with the formation of dianion TCNQ.

Table S3. Redox potential of $Mn^{III}PcQ^{-}$ and its precursors, Ep (V versus Ag/AgCl), ΔEp = Epf– Epb[V]. Conditions: 25 °C, working electrode: CPE modified by investigated compound [graphite + ionic liquid + compound ($Mn^{III}PcQ^{-}$ or MnPc or TCNQ)], Et_4NBF_4 background salt, CH_3CN,100 mV/s.

	$E_{1/2,}$ V	LUMO-1, eV HOMO-1, eV	GAP, eV
$Mn^{III}PcQ^{-}$			
R1	0.28	-4.63	0.65
R2	-0.21		
R3	-1.18		
R4	-1.62		
R5	-1.93		
O1	0.93	-5.28	
$Mn^{II}PC$			
R1	-0.29	-4.06	1.49
R2	-1.00		
R3	-1.38		
R4	-2.05		
O1	1.20		
O2	1.48		
O3	1.85	-5.55	
TCNQ			
R1	0.27	-4.62	-
R2	-0.22	-	